Influence of pyridazine derivative on corrosion inhibition of mild steel in acidic media

K. Benbouya, I. Forsal, M. Elbakri, T. Anik, R. Touir, M. Bennajah, D. Chebab, A. Rochdi, B. Mernari & M. Ebn Touhami

Research on Chemical Intermediates

ISSN 0922-6168

Res Chem Intermed
DOI 10.1007/s11164-013-1037-z

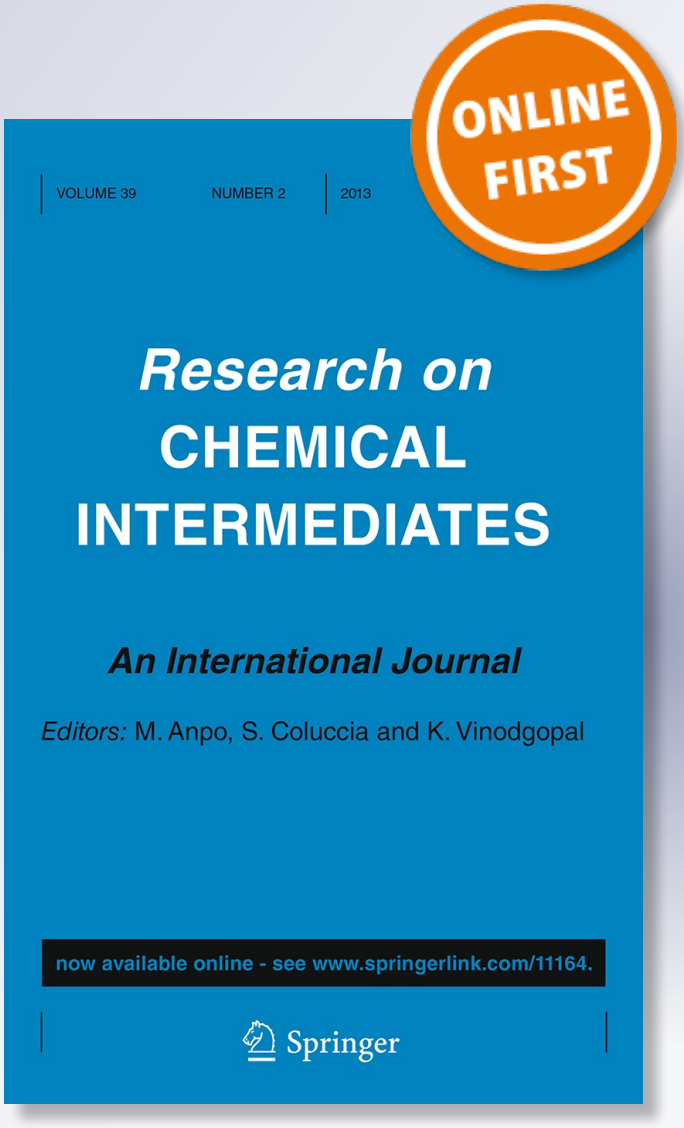

Springer

Res Chem Intermed
DOI 10.1007/s11164-013-1037-z

Influence of pyridazine derivative on corrosion inhibition of mild steel in acidic media

K. Benbouya · I. Forsal · M. Elbakri · T. Anik · R. Touir · M. Bennajah · D. Chebab · A. Rochdi · B. Mernari · M. Ebn Touhami

Received: 30 November 2012 / Accepted: 8 January 2013

Abstract The inhibition behavior of 6-methyl-4,5-dihydropyridazin-3(2H)-one (MDP) on corrosion of mild steel in 1 M HCl and 0.5 M H_2SO_4 was investigated using weight loss, potentiodynamic polarization, and electrochemical impedance spectroscopy (EIS) measurements. The results indicated that the corrosion inhibition efficiency depends on concentration, immersion time, solution temperature, and the nature of the acidic solutions. It is also noted that MDP is at its the most efficient in 1 M HCl and least in 0.5 M H_2SO_4. The effect is more pronounced with MDP concentration. It is found that the inhibition efficiency attains 98 % at 5×10^{-3} M in 1 M HCl and 75 % at 5×10^{-2} in 0.5 M H_2SO_4. Polarization measurements showed that the MDP acts as a mixed inhibitor. EIS diagrams showed that the adsorption of MDP increases the transfer resistance and decreases the capacitance of the interface metal/solution. From the temperature studies, the activation energies in the presence of MDP were found to be superior to those in uninhibited medium. Finally, a mechanism for the adsorption of MDP was proposed and discussed.

Keywords Corrosion inhibition · Mild steel · 1 M HCl · 0.5 M H_2SO_4 · EIS · Potentiodynamic polarization measurements · Pyridazine derivative

K. Benbouya · I. Forsal · M. Elbakri · T. Anik · R. Touir (✉) · D. Chebab · A. Rochdi · M. Ebn Touhami
Materials, Electrochemical and Environment Laboratory, Faculty of Science, Ibn Tofail University, BP 133, Kenitra, Morocco
e-mail: touir8@yahoo.fr

I. Forsal · B. Mernari
Coordination and Analytical Chemistry Laboratory, Faculty of Science, Chouaib Doukkali University, El Jadida, Morocco

M. Bennajah
Laboratoire de Génie des Procédés industriels, Ecole Nationale de l'industrie minérale, Av Haj Ahmed Cherkaoui, BP 753, Agdal, Rabat, Morocco

Published online: 23 January 2013

Introduction

Metals generally tend to move to their original state by corrosion processes. Mild steel is an alloy form of iron, which readily undergoes corrosion in acidic medium. Acidic solutions are extensively used in chemical laboratories and in several industrial processes such as acid pickling, acid cleaning, acid descaling, and oil wet cleaning, etc. [1–4]. Also, mild steel is used under different conditions in chemical and allied industries for handling alkaline, acid, and salt solutions. Chloride, sulfate, and nitrate ions in aqueous media are particularly aggressive and accelerate corrosion [5]. Most of the efficient inhibitors used in industry are organic compounds which mainly contain oxygen, sulfur, and nitrogen atoms and multiple bonds in the molecule through which they are adsorbed on the metal surface [6–18]. Moreover, many N-heterocyclic compounds have been proved to be effective inhibitors for the corrosion of metals and alloys in aqueous media [19–25].

This work deals with the study of the corrosion inhibition properties of 6-methyl-4,5-dihydropyridazin-3(2H)-one (MDP). The choice of this compound was based on the consideration that this compound contains π-electrons and heteroatoms such as N and O, which induce greater adsorption of the inhibitor molecule onto the surface of mild steel. The aim of this study was to determine the inhibition efficiency of MDP as a novel inhibitor for the corrosion of mild steel in 1 M HCl and 0.5 M H_2SO_4.

Experimental

Materials

Mild steel specimens of the following chemical composition (wt%) were used for the experiment: C = 0.11, Si = 0.24, Mn = 0.47, Cr = 0.12, Mo = 0.02, Ni = 0.1, Al = 0.03, Cu = 0.14, W = 0.06, Co < 0.0012, V < 0.003, and the remainder Fe. The structural formula of the commercial inhibitor is shown in Fig. 1. Its concentration was varied from 10^{-4} to 10^{-2} M. The electrolyte solutions of 1 M HCl and 0.5 M H_2SO_4 were prepared from commercial 37 % HCl and 98 % H_2SO_4, respectively, and distilled water.

Gravimetric measurements

The mild steel sheets of 2 cm × 2 cm × 0.05 cm were abraded with emery paper (grade from 400 to 1,200) and then washed with distilled water and acetone, and dried at room temperature. After weighing accurately, the specimens were

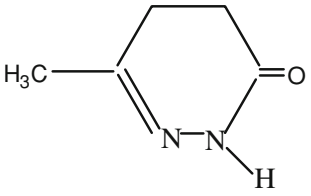

Fig. 1 Molecular structure of the inhibitor

immersed in corrosive medium with and without the addition of different concentrations of inhibitor for 6 h (the time which the inhibitor has its maximum inhibition for 1 M HCl). The mild steel sheets were then taken out, washed with distilled water and acetone, dried, and weighed accurately. The average weight loss of three substrate sheets could be obtained. The inhibition efficiency (η) values were calculated as follows:

$$\eta = \frac{\omega_0 - \omega}{\omega_0} \times 100 \tag{1}$$

where ω_0 and ω are the average weight loss values without and with inhibitor addition, respectively.

Electrochemical measurements

Electrochemical measurements were conducted in a conventional three-electrode cylindrical glass cell with a platinum as the counter electrode and a saturated calomel electrode (SCE) as the reference electrode. The working electrode was in the form of a square cut from mild steel embedded in epoxy resin of polytetrafluoroethylene so that the flat surface was the only surface in the electrolyte. The working surface area was 1 cm^2. The polarization curves were recorded by using a potentiostat/galvanostat (PGZ100). The potential increased with a speed of 1 mV/s and started from the potential of −750 to −100 mV/SCE for 1 M HCl and 0.5 M H_2SO_4. The temperature solution was fixed at 20 °C using a thermostat cell.

However, the overall current density, i, is considered as the sum of two contributions, anodic and cathodic current i_a and i_c respectively. For the potential domain not too far from the open circuit, we can consider that both processes obey the Tafel law [26], so we can draw:

$$i = i_a + i_b = i_{corr}.\{\exp[b_a \cdot (E - E_{corr})] - \exp[b_c \cdot (E - E_{corr})]\} \tag{2}$$

where i_{corr} is the corrosion current density (A cm^{-2}), and b_a and b_c are the Tafel constants of anodic and cathodic reactions (V^{-1}), respectively. These constants are related to the Tafel slope β (V/dec) in the usual logarithmic scale by:

$$b = \frac{\ln(10)}{\beta} \approx \frac{2.303}{\beta} \tag{3}$$

Corrosion parameters were then evaluated by the method of nonlinear least squares using Eq. (2). However, for this calculation, the applied potential range was limited to ± 0.100 V/SCE with respect to E_{corr} at which significant divergence has still sometimes been systematically observed for both anodic and cathodic branches.

The inhibition efficiency of inhibitor was calculated using the following equation:

$$\eta = \frac{i^0_{corr} - i_{corr}}{i^0_{corr}} \times 100 \tag{4}$$

where i^0_{corr} and i_{corr} are the corrosion rates in the absence and presence of inhibitor, respectively.

EIS measurements

The electrochemical impedance spectroscopy measurements were carried out using a transfer function analyzer (PGZ 100; Radiometer Analytical), with a small amplitude ac signal (10 mV rms), over a frequency range from 100 kHz to 10 mHz with ten points per decade. The impedance diagrams were given in the Nyquist presentation. To ensure reproducibility, all experiments were repeated three times and the evaluated inaccuracy does not exceed 10 %. The results were then analyzed using the Bouckamp program [27]. The inhibition efficiency was calculated using the following equation:

$$\eta = \frac{R_{ct} - R_{ct}^{0}}{R_{ct}} \times 100 \quad (5)$$

where R_{ct}^{0} and R_{ct} are the charge transfer resistance values without and with inhibitor, respectively.

Results and discussion

Gravimetric measurements

Table 1 shows the obtained results for mild steel in corrosive medium in the absence and presence of MDP at 293 K. It can be noted that the inhibition efficiency reached 98 % at 10^{-2} M of MDP and 55 % at 5×10^{-2} M of MDP in the case of 1 M HCl and 0.5 M H_2SO_4, respectively. As the corrosion rate decreased, the inhibition efficiency increased with MDP concentration in the test solution. This inhibition can be explained by the formation of a protective layer on the metallic surface through sharing electrons between nitrogen or oxygen and iron atoms.

However, the inhibition efficiency values are greater in the case of 1 M HCl than 0.5 M H_2SO_4. This is probably due to the lesser surface coverage in H_2SO_4 solution. Again, chloride ions have a greater adsorption tendency than sulfate ions on a mild steel surface [28].

Table 1 Inhibition efficiency for various concentrations of mild steel in 1 M HCl or 0.5 M H_2SO_4 obtained from weight loss measurements at 293 K after 6 h of immersion

	Concentration (M)	ω_{corr} (mg cm^{-2} h^{-1})	η (%)
1 M HCl	00	3.026	–
	10^{-4}	0.241	92
	10^{-3}	0.110	96
	5×10^{-3}	0.057	98
	10^{-2}	0.045	98
0.5 M H_2SO_4	00	7.243	–
	10^{-3}	5.728	21
	5×10^{-3}	4.657	35
	5×10^{-2}	3.237	55

Potentiodynamic polarization study

Figures 2 and 3 show potentiodynamic polarization curves for mild steel in 1 M HCl and 0.5 M H_2SO_4 with and without various concentration of MDP. It is noted that MDP suppressed the cathodic and anodic reactions. It is clear that the addition of MDP hindered the acid attack on the mild steel electrode, and a comparison of curves in both cases showed that, with respect to the blank, increasing the inhibitor concentration gave rise to a consistent decrease in anodic and cathodic current densities, indicating that MDP acts as a mixed-type inhibitor [29, 30].

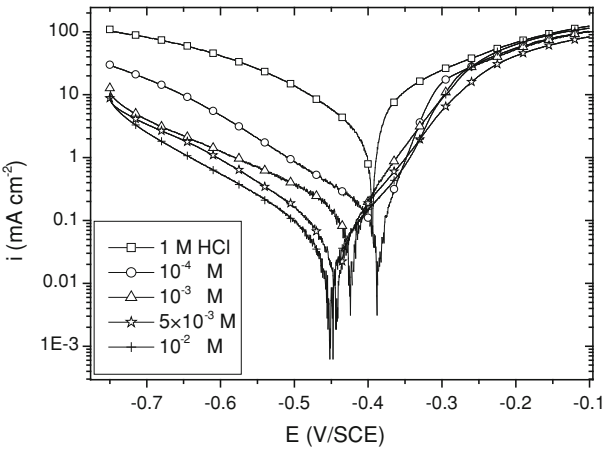

Fig. 2 Potentiodynamic polarization curves for mild steel in 1 M HCl containing different concentrations of MDP at 293 K

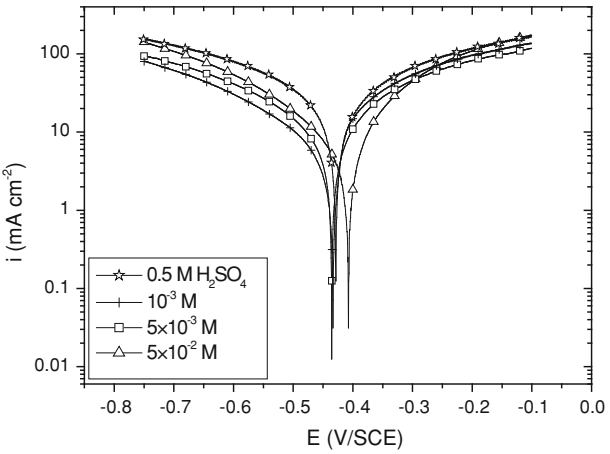

Fig. 3 Potentiodynamic polarization curves for mild steel in 0.5 M H_2SO_4 containing different concentrations of MDP at 293 K

However, i_{corr}, E_{corr} and b_c were evaluated from the experimental results using a user-defined function of "Non-linear least squares curve fit" (Eq. 2) of graphic software (Origin; OriginLab). In all cases, the correlation factor R^2 is greater than 0.99 indicating a reliable result. Figure 4 shows, as an example, the results of regressions calculation for the cathodic and anodic branches of mild steel in 1 M HCl in the presence of MDP at different concentrations. In this calculation, the potential domain is limited to $E_{corr} \pm 100$ mV as mentioned in our previous work [31]. A good agreementcan be seen in this figure between the calculated and the experimental polarization data.

Table 2 summarizes various corrosion kinetic parameters so obtained. It can be noticed that both anodic and cathodic current densities decrease gradually and the corrosion potential (E_{corr}) shifts slightly towards more negative values for increasing inhibitor concentrations. Analysis of these data shows that i_{corr} decreased with the addition of MDP in 1 M HCl and 0.5 M H_2SO_4. This can be explained by the increase in the blocked fraction of the electrode surface by adsorption.

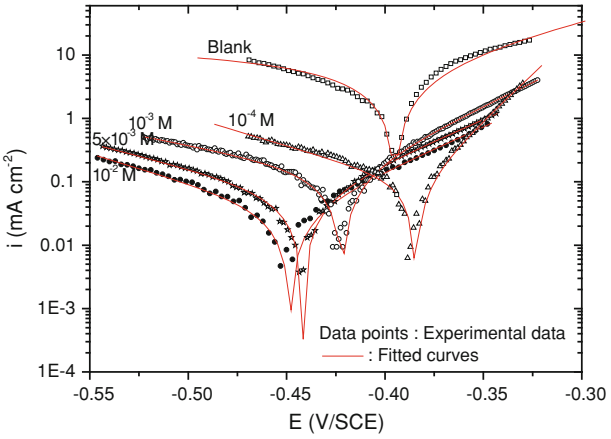

Fig. 4 Comparison of experimental and fitting data using a non-linear fitting with the Stern–Geary equation (case of HCl medium)

Table 2 Electrochemical parameters for mild steel in 1 M HCl or 0.5 M H_2SO_4 containing different concentrations of MDP at 293 K

	Concentration (M)	E_{corr} (mV/SCE)	i_{corr} (μA cm^{-2})	- β_c(V^{-1})	η (%)
1 M HCl	00	−396	1,072	2.36	–
	10^{-4}	−387	108	19.06	89
	10^{-3}	−424	84	13.56	92
	5×10^{-3}	−443	50	18.14	95
	10^{-2}	−453	31	21.19	97
0.5 M H_2SO_4	00	−409	4,843	4.64	–
	10^{-3}	−406	3,962	4.22	18
	5×10^{-3}	−410	2,485	1.06	49
	5×10^{-2}	−405	1,646	2.23	66

Electrochemical impedance spectroscopy study

The results described below can be interpreted in terms of the equivalent circuit of the double layer shown in Fig. 5, which has been used previously to model the iron–acid interface [30]. The corrosion behavior of mild steel in different corrosive media in the presence of various concentrations of MDP was investigated by EIS at 293 K. The obtained results are given in Figs. 6 and 7. As can be seen, in the presence of MDP the Nyquist plot always appears as a capacitive semicircle in the case of 1 M HCl, while in the case of 0.5 M H_2SO_4, a capacitive semicircle in the high to intermediate frequency range and an inductive loop in the low frequency range were observed. This last can be explained by the desorptions of MDP molecules. In addition, the impedance diagrams obtained were not perfect semicircles. This feature had been attributed to frequency dispersion [31]. It is apparent from these plots that the impedance response of mild steel in uninhibited 1 M HCl and 0.5 M H_2SO_4 solutions has significantly changed after the addition of MDP. This indicates that the impedance of the inhibited substrate increases with increasing inhibitor concentration in both acids.

The corrosion kinetic parameters such as charge transfer resistance (R_{ct}), double layer capacitance (C_{ct}), and inhibition efficiency (η) are given in Table 3. The greatest effect was observed at 10^{-2} M of MDP in 1 M HCl and at 5×10^{-2} M in 0.5 M H_2SO_4. It is seen that the C_{ct} values decrease with the concentration of the

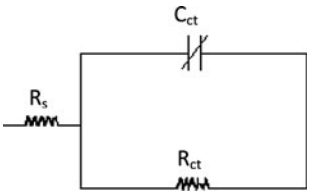

Fig. 5 Electrical equivalent circuit for the metal–acid interface

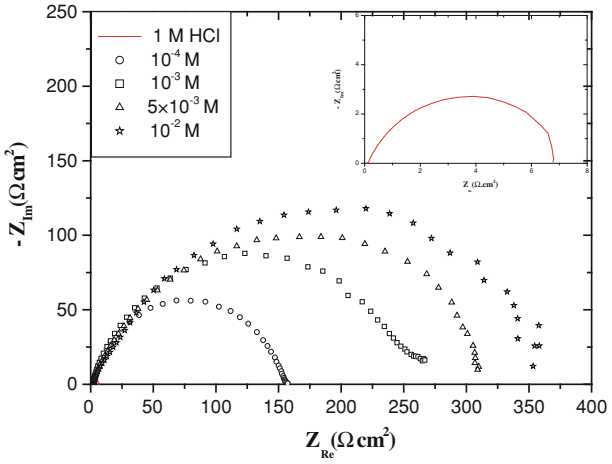

Fig. 6 Nyquist plots for mild steel in 1 M HCl containing different concentrations of MDP at 293 K

inhibitor. The decrease in the C_{ct}, which can result from the decrease in the local dielectric constant and/or an increase in the thickness of the electrical double layer, suggested that the MDP molecules function by adsorption at the metal–solution interface [32, 33]. Similar behavior was observed in both media [30].

It is well known that the inhibitive action of organic compounds containing S, N and/or O is due to the formation of a co-ordinate-type bond between the metal and the lone pair of electrons in the additive. The tendency to form a co-ordinate bond and hence the extent of inhibition can be enhanced by increasing the effective electron density at the functional group of the additive [34]. In aromatic or hyterocyclic ring compounds, the effective electron density at the functional group can be varied by introducing different substituents in the ring leading to variations of the molecules' structure.

The adsorption of MDP on the metal surface can occur either directly on the basis of donor–acceptor interactions between the π-electrons of the inhibitor and the

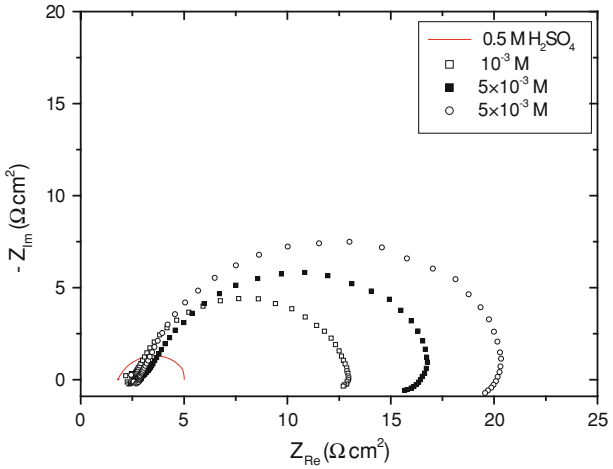

Fig. 7 Nyquist plots for mild steel in 0.5 M H_2SO_4 containing different concentrations of MDP at 293 K

Table 3 Data obtained from EIS measurements for mild steel in 1 M HCl or 0.5 M H_2SO_4 in the presence of different concentrations of MDP

	Concentration (M)	R_{ct} (Ω cm^2)	C_{ct} (μF cm^{-2})	η (%)
1 M HCl	00	6.8	165	–
	10^{-4}	156	12	96
	10^{-3}	270	8	97
	5×10^{-3}	309	7	98
	10^{-2}	350	7	98
0.5 M H_2SO_4	00	5	168	–
	10^{-3}	13	56	61
	5×10^{-3}	17	48	70
	5×10^{-2}	20	35	75

vacant d-orbitals of iron surface atoms. or through an interaction of the inhibitor with the already adsorbed sulfate or chlorure ions [35, 36].

Effect of temperature

The temperature effect on inhibition efficiency was determined in 1 M HCl and 0.5 M H_2SO_4 containing 10^{-2} M and 5×10^{-2} of MDP in the temperature range 293–323 K in both solutions using potentiodynamic polarization curves. The obtained results are given in Table 4. As expected, the corrosion current densities increased by one order of magnitude with increasing temperature both in uninhibited and inhibited solutions. Thus, the inhibition efficiency values of MDP were slightly decreased in the temperature range as a result of the higher dissolution of mild steel at higher temperatures. This might be caused by the desorption of MDP from the mild steel surface.

Corrosion current densities for mild steel increased more rapidly with temperature in the absence of the inhibitor (blank solution). These results confirmed that the MDP acts as an efficient inhibitor in the range of temperature studied. The apparent activation energy values E_a were calculated from the Arrhenius equation:

$$i_{corr} = K \exp\left(-\frac{E_a}{RT}\right) \quad (6)$$

where i_{corr} is the corrosion current density, K is the Arrhenius pre-exponential factor, T is the absolute temperature, and R is the universal gas constant.

Table 4 Influence of temperature on the electrochemical parameters for a mild steel electrode immersed in corrosive media containing MDP

	Temperature (K)	E_{corr} (mV/SCE)	i_{corr} (μA cm^{-2})	η (%)
Blank solution 1 M HCl	293	−396	1,072	–
	303	−395	1,664	–
	313	−396	2,158	–
	323	−404	2,743	–
10^{-2} of MDP	293	−453	31	99
	303	−417	66	96
	313	−398	166	92
	323	−398	408	85
Blank solution 0.5 M H_2SO_4	293	−409	4,843	–
	303	−434	5,630	–
	313	−440	6,888	–
	323	−426	8,705	–
5×10^{-2} M of MDP	293	−405	1,646	66
	303	−436	3,159	43
	313	−430	4,680	32
	323	−428	6,735	23

The Arrhenius plot according to Eq. (6) is shown in Figs. 8 and 9. The obtained plots were straight lines and the E_a values were found equal to 23 and 15.4 kJ mol^{-1} in 1 M HCl and 0.5 M H_2SO_4, respectively. In the presence of MDP, which functions as an effective inhibitor, the E_a values are higher and equal to 68 kJ mol^{-1} in 1 M HCl and 36.54 kJ mol^{-1} in 0.5 M H_2SO_4. According to Gomma [37], the kinetic of such a corrosion process acquires the character of a diffusion process in which at lower temperatures the quantity of the inhibitor present at the metal surface is greater than that at higher temperatures. The negative slope of E_a indicates the adsorption of the organic compound on the electrode surface [38].

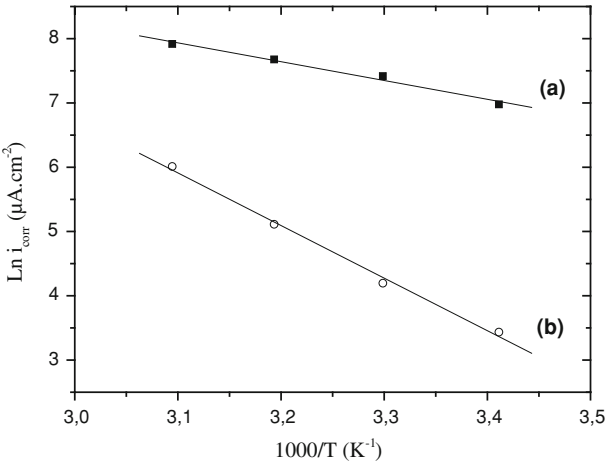

Fig. 8 Arrhenius plot of i_{corr} with respect to the T: **a** 1 M HCl and **b** 1 M HCl + 10^{-2} M of MDP

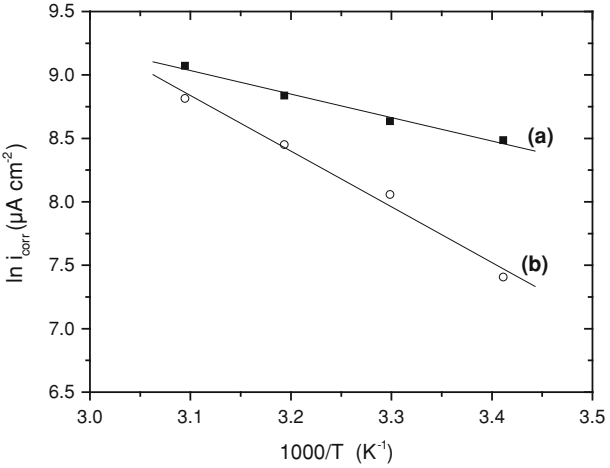

Fig. 9 Arrhenius plot of i_{corr} with respect to the T: **a** 0.5 M H_2SO_4 and **b** 0.5 M H_2SO_4 + 5 × 10^{-2} M of MDP

In addition, we also noted that the apparent activation energy values in the presence of MDP are greater than those obtained in its absence. This can be explained by the way that the MDP acts by physical adsorption [20, 39].

Immersion time

Figures 10 and 11 show the impedance spectra at different immersion times in 1 M HCl and 0.5 M H_2SO_4 in the presence of MDP at the optimum concentration. It is noticeable that these diagrams exhibit one capacitive loop. It is also of note that an inductive loop in the low frequency range was observed in the case of 0.5 M H_2SO_4.

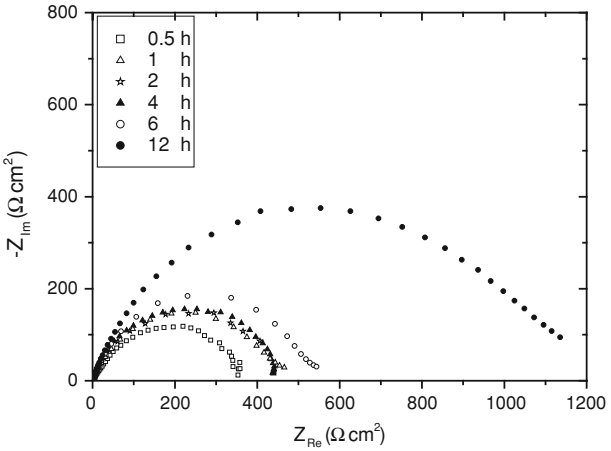

Fig. 10 Nyquist diagrams for mild steel in 1 M HCl containing 10^{-2} M of MDP at different immersion times over open circuit potential

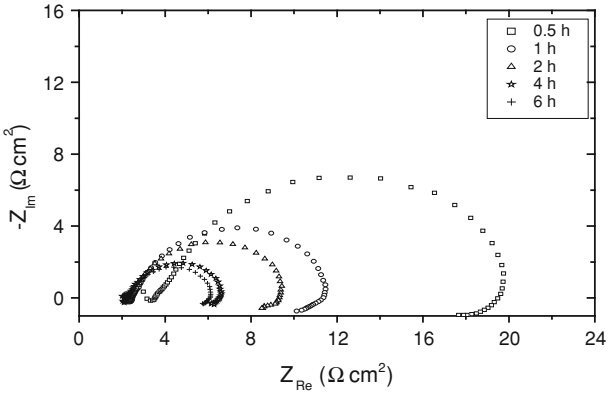

Fig. 11 Nyquist diagrams for mild steel in 0.5 M H_2SO_4 containing 5×10^{-2} M of MDP at different immersion times over open circuit potential

Table 5 Influence of immersion time on the electrochemical parameters for mild steel in corrosive media + MDP

	Immersion time (h)	R_{ct} (Ω cm^2)	C_{ct} (μF cm^{-2})	η (%)
1 M HCl + 10^{-2} M of MDP	1/2	350	7	97
	1	447	6	98
	2	448	6	98
	4	449	6	98
	6	520	6	98
	12	1,160	5	99
0.5 M H_2SO_4 + 5 × 10^{-2} M of MDP	1/2	20	35	75
	1	11.5	47	56
	2	9.5	55	47
	4	6.6	59	24
	6	6.1	59	18

The evolution of the characteristics parameters associated with the capacitive loop with time is summarized in Table 5.

In the case of H_2SO_4, The diameter of the capacitive loop decreases in size with immersion time. These results indicate that the adsorption model, and the arrangement and orientation of MDP on the surface of the mild steel, change with time.

In the case of HCl, the diameter of the capacitive loop increases in size with immersion time. These results indicate that the immersion time increases the chloride quantity which will be adsorbed on the surface, helping in the formation of the inhibitor layer. However, the entire active sites become saturated with inhibitor molecules. Furthermore, the change in the C_{ct} values may be caused by the gradual replacement of water molecules by the chloride anion, and by the adsorption of the organic molecules on the metal surface, decreasing the extent of the dissolution reaction.

This difference in the inhibition in both acids can be explained by in the case of H_2SO_4, $FeSO_4$ being less soluble than $FeCl_2$ and staying more efficiency on the steel surface. Fewer organic molecules are chemisorbed and, therefore, C_{ct} values are more important [40, 41].

Adsorption mechanism

From the above finding, we can say that MDP is adsorbed on mild steel. As far as the inhibition process is concerned, it is generally assumed that the adsorption of the inhibitor at the metal–solution interface is the first step in the action mechanism of inhibitors in aggressive acid media. Four types of adsorption may take place involving organic molecules at the metal–solution interface: (1) electrostatic attraction between charged molecules and the charged metal, (2) interaction of unshared electron pairs in the molecules with the metal, (3) interaction of π-electrons with the metal, and (4) a combination of the above [42].

Chemisorption involves charge sharing or charge transfer from the inhibitor molecules to the surface to form a coordinate-type bond. In fact, electron transfer is typical for transition metals having vacant, low-energy electron orbitals. Electron

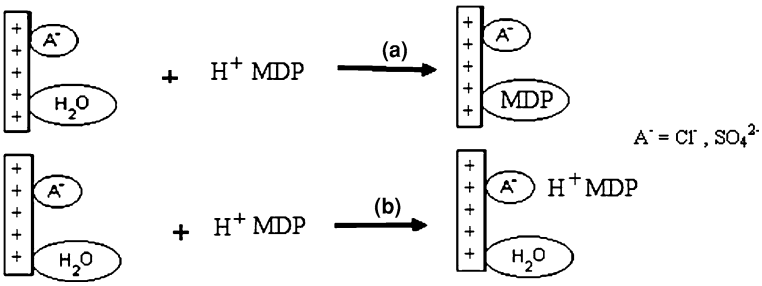

Fig. 12 Schematic representations of **a** competitive and **b** cooperative adsorption of MDP in acid solutions

transfer can be expected with compounds having relatively loosely bound electrons [43]. Inhibition efficiency depends on several factors, such as the number of adsorption sites and their charge density, molecules size, heat of hydrogenation, mode of interaction with the metal surface, and the formation of metallic complexes [44]. Most organic compounds contain at least one polar group with an atom of nitrogen, sulfur or oxygen; each of them might be a chemisorption center. The inhibitive proprieties of such compounds depend on the electron densities around the chemisorptions center; the more the effect, the more inhibition.

The following explanations are postulated: MDP interferes in the dissolution reaction by adsorption at the metal surface in two deferent ways. First, the inhibitor competes with Cl^{-} or SO_4^{2-} ions for sites at the water covered anodic surface. In doing so, the protonated inhibitor loses its associated proton(s) in entering the double layer and chemisorbed by donating electrons to the metal. In addition, the protonated inhibitor electrostatically adsorbs onto the anion-covered surface through its cationic form. Bode modes of adsorption are depicted in Fig. 12. MDP thus plays a dynamic role at the interface and interferes with dissolution reaction by participating in a number of adsorption–desorption steps, rather than solely by a blockage of sites [35, 45, 46]. Iron sites covered by adsorbed inhibitor molecules (competitive or cooperative adsorption) are dissolution precursors. A similar mechanism was proposed by Bentiss et al. [30].

Conclusion

(1) The MDP shows good inhibiting properties for mild steel in both media in 1 M HCl.
(2) In both media, this compound was found to affect the anodic and cathodic processes and acts as a mixed-type inhibitor.
(3) Based on the apparent activation energy values, the MDP acts by physical adsorption.
(4) Inhibition efficiency is greater in the case of 1 M HCl than 0.5 M H_2SO_4.
(5) The inhibition efficiency increases with immersion time. In the case of HCl, this study indicates that the MDP inhibitor was strongly adsorbed on the mild steel surface.

References

1. M. Dahmani, A. Et-Touhami, S.S. Al-Deyab, B. Hammouti, A. Bouyanzer, Int. J. Electrochem. Sci. **5**, 1060 (2010)
2. B.M. Praveen, T.V. Venkatesha, Int. J. Electrochem. Sci. **4**, 267–275 (2009)
3. D. Chebabe, Z. Ait Chikh, N. Hajjaji, Corros. Sci. **45**, 309–320 (2003)
4. J.M. Bastidas, J.L. Polo, E. Cano, J. Electrochem. Soc. **30**, 1173 (2000)
5. F. Bentiss, M. Lagrenée, M. Traisnel, B. Mernari, H. El Attari, J. Appl. Electrochem. **29**, 1073 (1999)
6. M. Benabdellah, R. Touzani, A. Dafali, B. Hammouti, S. El Kadiri, Mater. Lett. **61**, 1197–1204 (2007)
7. M. Benabdellah, A. Aouniti, A. Dafali, B. Hammouti, M. Benkaddour, A. Yahyi, A. Ettouhami, Appl. Surf. Sci. **252**, 8341–8347 (2006)
8. B. Zerga, B. Hammouti, M. Ebn Touhami, R. Touir, M. Taleb, M. Sfaira, M. Bennajeh, I. Forssal, Int. J. Electrochem. Sci. **7**, 471–483 (2012)
9. L. Wang, Corros. Sci. **48**, 608–616 (2006)
10. Y. Aouine, M. Sfaira, M. Ebn Touhami, A. Alami, B. Hammouti, M. Elbakri, A. El Hallaoui, R. Touir, Int. J. Electrochem. Sci. **7**, 5400–5419 (2012)
11. M. Lebrini, F. Bentiss, H. Vezin, M. Lagrenée, Corros. Sci. **48**, 1279 (2006)
12. K. Adardour, R. Touir, Y. Ramli, R.A. Belakhmima, M.E. Touhami, C.K. Mubengayi, H. El Kafsaoui, E.M. Essassi, Res. Chem. Intermed. (2012). doi:10.1007/s11164-012-0719-2
13. A. Lamkaddem, R. Touir, E.M. Essassi, M. Ebntouhami, Scientific study et research, Vol. VIII(1) (2007). ISSN 1582-540X
14. M. Lebrini, M. Lagrenée, H. Vezin, L. Gengembre, F. Bentiss, Corros. Sci. **47**, 485 (2005)
15. G. Gunasekaran, L.R. Chauhan, Electrochim. Acta **49**, 4387–4439 (2004)
16. M.A. Quraishi, J. Rawat, Mater. Chem. Phys. **73**, 118–122 (2002)
17. L. Wang, Corros. Sci. **43**, 1637–1644 (2001)
18. R. Hardre, C. Bonnette, L. Salmon, A. Gaudemer, Bioorg. Med. Chem. Lett. **8**, 3435–3438 (1998)
19. Y. Abboud, A. Abourriche, T. Saffaj, M. Berrada, M. Charrouf, A. Bennamar, N. Al Himidi, H. Hannache, Mater. Chem. Phys. **105**, 1–5 (2007)
20. M. Elbakri, R. Touir, M. Ebn Touhami, A. Zarrouk, Y. Aouine, M. Sfaira, M. Bouachrine, A. Alami, A. El Hallaoui, Res. Chem. Intermed. (2012). doi:10.1007/s11164-012-0768-6
21. K. Aderdour, R. Touir, M. Ebn Touhami, M. Sfaira, H. El Kafssaoui, B. Hammouti, H. Benzaid, M. El Essassi, Der Pharma Chemica **4**, 1485–1495 (2012)
22. J. Hmimou, A. Rochdi, R. Touir, M. Ebn Touhami, E.H. Rifi, A. El Hallaoui, A. Anouar, D. Chebab, J. Mater. Environ. Sci. **3**, 543–550 (2012)
23. Y. Elkacimi, M. Achnin, Y. Aouine, M. Ebn Touhami, A. Alami, R. Touir, M. Sfaira, D. Chebabe, A. Elachqar, B. Hammouti, Portugaliae Electrochimica Acta **30**, 53–65 (2012)
24. M. Mihit, S. El Issami, M. Bouklah, L. Bazzi, B. Hammouti, E. Ait Addi, R. Salghi, S. Kertit, Appl. Surf. Sci. **252**, 2389 (2006)
25. K. Adardour, O. Kassou, R. Touir, M. Ebn Touhami, H. ElKafsaoui, H. Benzeid, El M. Essassi, M. Sfaira, J. Mater. Environ. Sci. **1**, 129–138 (2010)
26. M. Stern, A.L. Geary, J. Electrochem. Soc. **104**, 56–63 (1957)
27. A. Boukamp, *Users Manual Equivalent Circuit, ver. 4.51*, (1993)
28. R.A. Prabhu, A.V. Shanbhag, T.V. Venkatesha, J. Appl. Electrochem. **37**, 491 (2007)
29. S. Muralidharan, K.L.N. Phani, S. Pitchumani, S. Ravichandran, S.V.K. Iyer, J. Electrochem. Soc. **142**, 1478 (1995)
30. F. Bentiss, M. Traisnel, M. Lagrenée, J. Appl. Electrochem. **31**, 41–48 (2001)
31. A. Majjane, D. Rair, A. Chahine, M. Et-tabirou, M. Ebn Touhami, R. Touir, Corros. Sci. **60**, 98–103 (2012)
32. F. Mansfeld, Corrosion **36**, 301 (1981)
33. F. Mansfeld, M.W. Kendig, S. Tsai, Corrosion **38**, 570 (1982)
34. J.G.N. Thomas, in *"Corrosion"*, 2nd edn, Vol. 2, chapter 18, ed. by L.L. Shereir (Newness-Butterworths, London, 1979)
35. N. Hackerman, E.S. Snavely, J.S. Payene, J. Electrochem. Soc. **113**, 677 (1966)
36. S. Tamil selvi, V. Raman, N. Rajendran, J. Appl. Electrochem. **33**, 1175–1182 (2003)
37. G.K. Gomma, Mater. Chem. Phys. **55**, 131 (1998)
38. V. Branzoi, F. Branzoi, M. Baibarac, Mater. Chem. Phys. **65**, 288 (2000)

39. F. Bentiss, M. Traisnel, L. Genegembre, M. Lagrene′e, Appl. Surf. Sci. **152**, 237 (1999)
40. L. Klkadi, B. Mernari, M. Trainsel, F. Bentiss, M. Lagrenée, Corros. Sci. **42**, 703 (2000)
41. M. Lagrenée, B. Mernari, M. Bouanis, M. Trainsel, F. Bentiss, Corros. Sci. **44**, 573–588 (2002)
42. D. Schweinsberg, G. George, A. Nanayakkara, D. Steiner, Corros. Sci. **28**, 33 (1988)
43. F. Mansfeld, *Corrosion Inhibitors* (Marcel Dekker, New York, 1987), p. 119
44. A. Fouda, M. Moussa, F. Taha, El Neanaa, Corros. Sci. **26**, 719 (1986)
45. N. Hackerman, E. McCafferty, *Proceedings of the 5th International Congress on 'Metallic Corrosion'* (Tokyo, 1972) p. 542
46. T. Murakawa, N. Hackerman, Corros. Sci. **4**, 387 (1964)